COMMUNICATION

Optically-pure triptycene-based metallomacrocycles and homochiral self-sorting assisted by ladder formation†
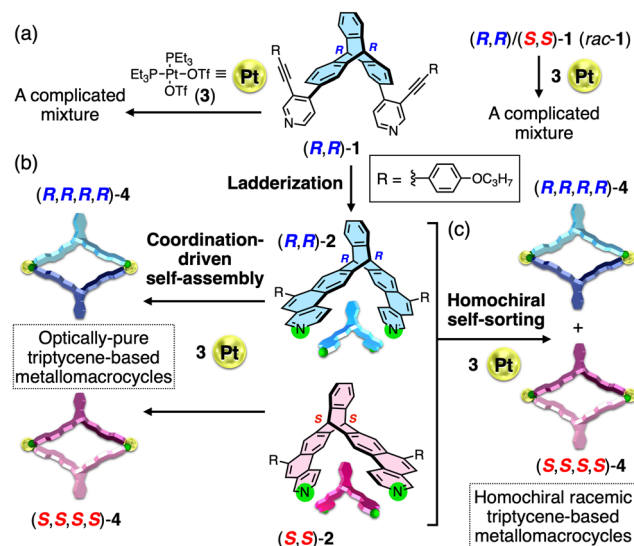
Kosuke Oki, ‡[a] Wei Zheng, ‡§[a] Eiji Yashima [a] and Tomoyuki Ikai ⋆[ab]

Optically-pure triptycene-based metallomacrocycles are, for the first time, synthesized by the coordination-driven self-assembly of enantiopure triptycene-derived ladder-type bis(benzo[f]isoquinoline) ligands with a cis-platinum(II) complex. A pair of enantiomeric homochiral metallomacrocycles is also produced by the coordination-driven homochiral self-sorting of the corresponding racemic ligands, which relies on the shape-persistent nature of the ladder-structured ligands.

The pristine triptycene is a rigid and bulky achiral aromatic hydrocarbon with D_{3h}-symmetry,[1] but its derivatives become chiral when substituents are introduced in an asymmetric fashion as first reported by Sonoda *et al.* in 1962.[2] In spite of the unique chiral framework of the substituted chiral triptycenes, however, the application of optically-active triptycenes as chiral functional materials has received little or no attention until the late 2010s. The groups of Chen, Fukushima, and Ikai have demonstrated the potential of optically-active triptycenes as a promising chiral scaffold for applications in chiral recognition,[3] asymmetric catalysis,[4] enantioseparation,[5,6] and circularly polarized luminescence (CPL).[7–9] Since then, the synthesis and applications of optically-active triptycenes have attracted ever-increasing attention.[10–12] In terms of the rational design and construction of three-dimensional (3D) chiral nanostructures, the triptycene framework is very attractive, because its conformational freedom is highly restricted due to its robust 3D paddlewheel-like shape, which strictly defines the directionality of covalent bonds and overall spatial geometry of molecules, supramolecules, and polymers. In fact, covalently-bonded homochiral organic macrocycles/cages[11,13] and one-handed helical polymers[6] have been successfully synthesized using optically-pure triptycenes as a key chiral framework. However, despite their high structural designability, to the best of our knowledge, chiral triptycene-based optically-pure metallomacrocycles have never been reported. (For examples of triptycene-based optically-inactive metallomacrocycles composed of achiral or racemic building blocks, see: ref. 14–21.)

Homochiral self-sorting is a unique phenomenon probably related to the origin of biological homochirality, in which

a Department of Molecular and Macromolecular Chemistry, Graduate School of Engineering, Nagoya University, Chikusa-ku, Nagoya 464-8603, Japan.
E-mail: ikai@chembio.nagoya-u.ac.jp
b Precursor Research for Embryonic Science and Technology (PRESTO), Japan Science and Technology Agency (JST), Kawaguchi, Saitama 332-0012, Japan

† Electronic supplementary information (ESI) available: Experimental procedures, characterizations, and additional supporting data. CCDC 2258185. For ESI and crystallographic data in CIF or other electronic format see DOI: https://doi.org/10.1039/d3cc02259e

‡ These authors contributed equally to this work.

§ Present address: College of Materials Science and Engineering, Tongji University, Shanghai, 201804, China.

Fig. 1 (a) Coordination-driven self-assembly of (R,R)- and racemic-triptycene-derived non-ladder-type bispyridine ligands ((R,R)-**1** (left) and (R,R)/(S,S)-**1** (rac-**1**) (right)) with a 90° platinum(II) complex (cis-Pt(PEt₃)₂(OTf)₂ (**3**)). (b and c) Schematic illustrations of the synthesis of optically-pure triptycene-based metallomacrocycles ((R,R,R,R)- and (S,S,S,S)-**4**) by the coordination-driven self-assembly of optically-pure triptycene-derived ladder-type bis(benzo[f]-isoquinoline) ligands ((R,R)- and (S,S)-**2**) with **3** (b) and the homochiral self-sorting of the corresponding racemic ligand ((R,R)/(S,S)-**2** (rac-**2**)) into a pair of enantiomeric homochiral metallomacrocycles ((R,R,R,R)/(S,S,S,S)-**4** (rac-**4**)) (c).

homochiral species spontaneously assemble with each other in preference to heterochiral assembly by stronger homochiral interactions primarily through metal coordination and hydrogen bonding, and has been observed in a variety of chiral molecules.[22–27] However, there is no precedent for the homochiral self-sorting of racemic triptycenes.[28]

We now report the first synthesis of optically-pure triptycene-based metallomacrocycles ((R,R,R,R)- and (S,S,S,S)-4) formed by the coordination-driven self-assembly of optically-pure triptycene-derived ladder-type bis(benzo[f]isoquinoline) ligands ((R,R)- and (S,S)-2) with an equivalent amount of a 90° platinum(II) complex (cis-Pt(PEt$_3$)$_2$(OTf)$_2$ (3))[29] (Fig. 1b). We found that the shape-persistent ladder structure of the triptycene ligands ((R,R)- and

(S,S)-2) obtained after versatile acid-promoted alkyne benzannulations of the corresponding precursor ligands ((R,R)- and (S,S)-1)[6,30,31] enabled the quantitative and selective formation of the Pt$_2$L$_2$-type metallomacrocycles (Fig. 1a and b), whereas the precursor ligands bearing two flexible pyridyl groups as the metal-binding sites afforded a complicated oligomeric mixture upon mixing with 3. Moreover, we report a first homochiral self-sorting of a racemic triptycene ligand ((R,R)- and (S,S)-2 (rac-2)) with 3, thus producing a pair of enantiomeric homochiral triptycene-based metallomacrocycles ((R,R,R,R)/(S,S,S,S)-4 (rac-4)) (Fig. 1c).

We first synthesized the optically-pure ((R,R)- and (S,S)-1) and racemic (rac-1) triptycene-based precursors containing 2-[(p-propoxyphenyl)ethynyl]-4-pyridyl groups at the 2,6-positions of
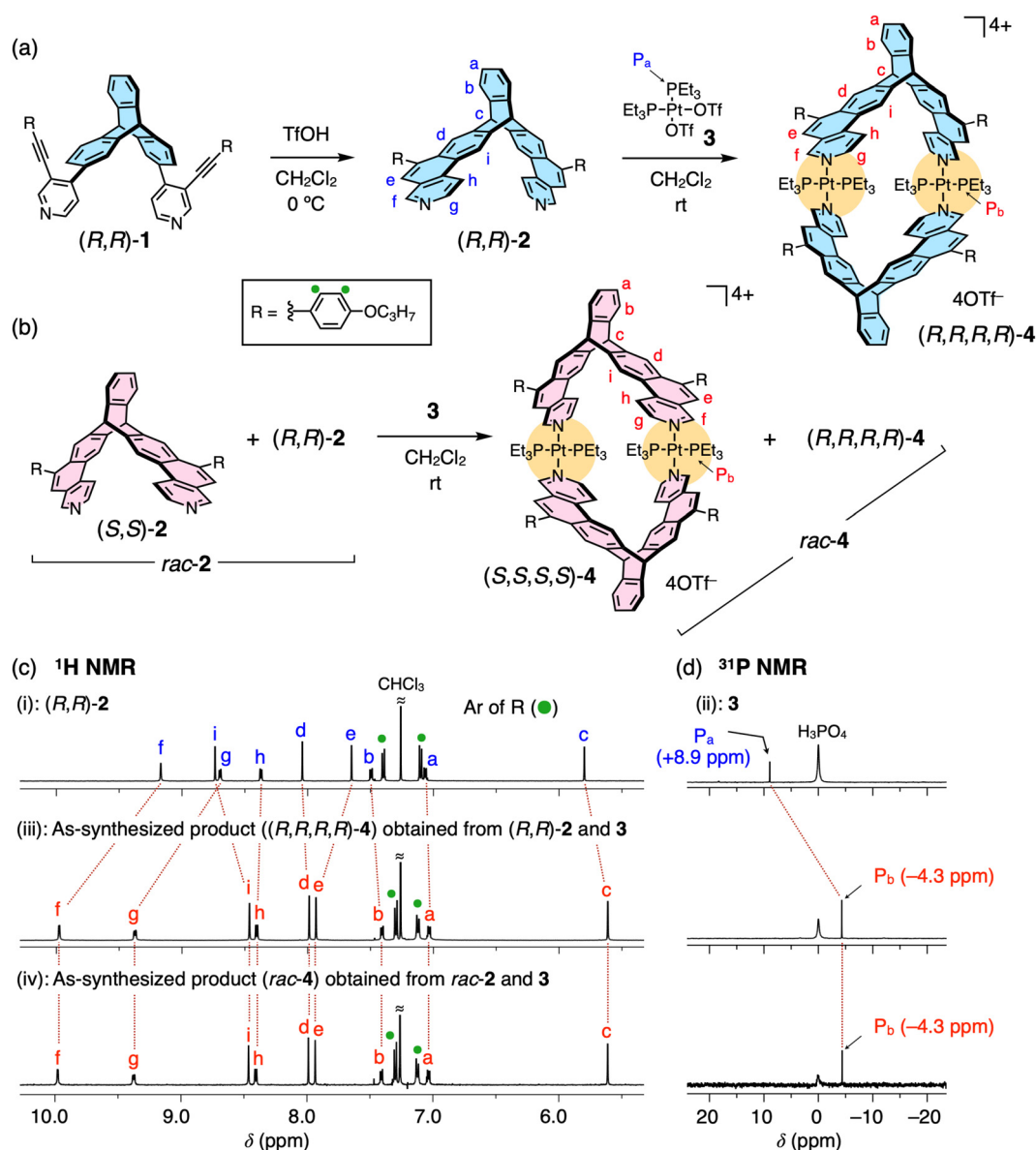
Fig. 2 (a and b) Synthesis of optically-pure (a; (R,R,R,R)-4) and racemic (b; rac-4) homochiral triptycene-based metallomacrocycles by the coordination-driven self-assembly of (R,R)-2 and rac-2 with cis-Pt(PEt$_3$)$_2$(OTf)$_2$ (3), respectively. (c and d) ^{1}H (c; 500 MHz, CDCl$_3$, 25 °C) and/or ^{31}P (d; 203 MHz, CDCl$_3$, room temperature) NMR spectra of (R,R)-2 (i), 3 (ii), and the as-synthesized products ((R,R,R,R)-4 (iii) and rac-4 (iv)) obtained through complexation reaction of (R,R)-2 and rac-2 with 3, respectively. For the signal assignments of (c), see Fig. S2 (ESI†).

the triptycene unit by Suzuki–Miyaura coupling according to Scheme S1 (ESI†). The subsequent acid-promoted alkyne benzannulations[6,30,31] with trifluoromethanesulfonic acid (TfOH) quantitatively produced (*R*,*R*)-, (*S*,*S*)-, and *rac*-**2** in a complete regioselective manner, respectively (Scheme S1 and Fig. S1, ESI†).

When (*R*,*R*)-**2** was allowed to react with an equimolar amount of **3** in dichloromethane at room temperature for 3 h (Fig. 2a and Scheme S2, ESI†), the complexation reaction completely proceeded, quantitatively affording the single (*R*,*R*)-**2**-platinum(II) complex with a highly symmetric structure, as supported by the simple ¹H and ³¹P NMR spectra of the as-synthesized product (Fig. 2c and d(iii)); a new set of proton resonances and one phosphorus peak being significantly different from those of (*R*,*R*)-**2** (Fig. 2c(i)) and **3** (Fig. 2d(ii)), respectively, were observed. In contrast, the ¹H and ³¹P NMR spectra of the reaction products of the precursor ligand ((*R*,*R*)-**1**) with **3** were complicated, indicating the formation of various by-products including cyclic and non-cyclic oligomers (Fig. S3a, b(i, ii) and S4, ESI†). The high-resolution electrospray ionization mass (ESI-MS) analysis of the as-synthesized (*R*,*R*)-**2**-platinum(II) complex revealed the Pt₂L₂-type metallomacrocycle ((*R*,*R*,*R*,*R*)-**4**) formation, showing two characteristic molecular peaks at *m*/*z* of 577.7274 and 819.9560 corresponding to the [**4**–4OTf⁻]⁴⁺ and [**4**–3OTf⁻]³⁺ species, respectively (Fig. S5a(i, ii), ESI†). These peaks agreed well with the simulated ones. The (*S*,*S*)-**2**-platinum(II) complex ((*S*,*S*,*S*,*S*)-**4**) was also prepared in the same way (Scheme S2, ESI†).

Single crystals of the (*R*,*R*)- and (*S*,*S*)-**2**-platinum(II) complexes suitable for X-ray analysis could not be obtained despite various attempts, but X-ray-quality crystals were successfully obtained from the reaction product of *rac*-**2** (an equimolar mixture of (*R*,*R*)-**2** and (*S*,*S*)-**2**) and **3** (Fig. 2b). The single-crystal X-ray crystallographic analysis of *rac*-**4** unambiguously revealed the Pt₂L₂-type rhombic metallomacrocycle structure composed of two homochiral triptycene units, namely, (*R*,*R*,*R*,*R*)- and (*S*,*S*,*S*,*S*)-**4** (Fig. 3), which were exclusively formed from *rac*-**2** and **3** via a complete homochiral self-sorting,[22–28] as supported by the identical ¹H and ³¹P NMR and ESI-MS spectra to those of the as-synthesized product ((*R*,*R*,*R*,*R*)-**4**) from (*R*,*R*)-**2** and **3** (Fig. 1c, 2c, d, and Fig. S5, ESI†). The steric effect between the 4-propoxyphenyl (R) pendants most likely provides a crucial difference in the thermodynamic stability of (*R*,*R*,*R*,*R*)- and (*R*,*R*,*S*,*S*)-**4** (for the DFT calculation results, see Fig S6, ESI†). In the crystal packing structure, (*R*,*R*,*R*,*R*)- and (*S*,*S*,*S*,*S*)-**4** are separately stacked to form the corresponding homochiral columnar structures along the *b* axis (Fig. 3b). The distances between the two centroids of the triptycene units and between the two platinum atoms are 10.2 and 17.0 Å, respectively (Fig. 3a(ii)). As anticipated, such a self-sorting did not occur when *rac*-**1** was mixed with **3** (Fig. S3a, b(iii, iv), ESI†). These results indicated the crucial role of the rigid ladder-structured ligand **2**, in which the two metal-binding sites of **2** are preorganized to coordinate to the platinum(II) ions, leading to the quantitative and selective formation of the Pt₂L₂-type homochiral triptycene-based metallomacrocycles.

As shown in Fig. 4, the (*R*,*R*,*R*,*R*)- and (*S*,*S*,*S*,*S*)-**4** metallomacrocycles exhibited absorption bands in a longer wavelength
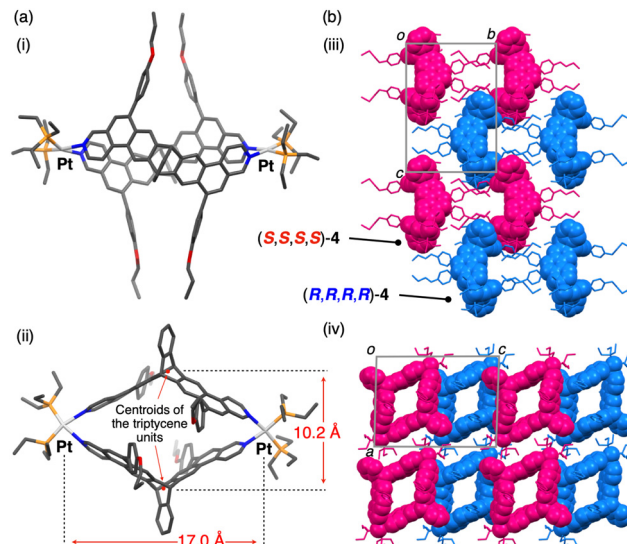

Fig. 3 (a) Perspective view of the crystal structure of *rac*-**4** (top (i) and side (ii) views). The distances between the two centroids of the triptycene units and between the two platinum atoms are also shown. (b) Crystal packing structure of (*R*,*R*,*R*,*R*)/(*S*,*S*,*S*,*S*)-**4** (*rac*-**4**) as viewed along the *a* (iii) and *b* (iv) axes of the unit cell shown in gray. The structures are represented by space-filling models except for the 4-propoxyphenyl pendant groups and the triethylphosphine ligands, which are shown as capped-stick ones, and enantiomeric frameworks of (*R*,*R*,*R*,*R*)- and (*S*,*S*,*S*,*S*)-**4** are colored in blue and pink, respectively. All the hydrogen atoms, solvent molecules, and disordered atoms are omitted for clarity.
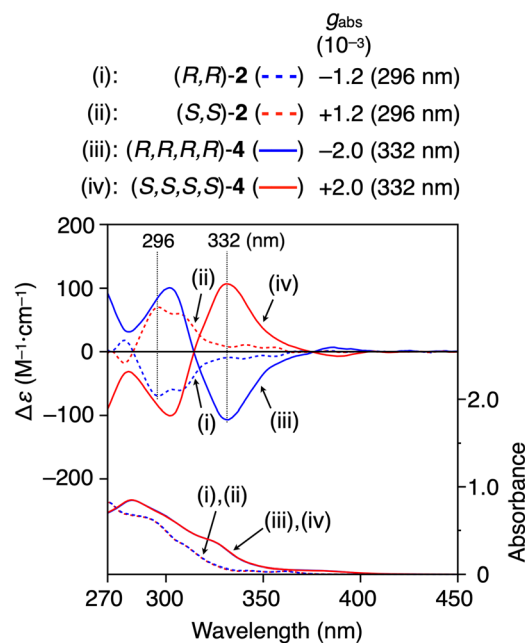

Fig. 4 CD and absorption spectra of (*R*,*R*)-**2** (i), (*S*,*S*)-**2** (ii), (*R*,*R*,*R*,*R*)-**4** (iii), and (*S*,*S*,*S*,*S*)-**4** (iv) in chloroform at 25 °C. [**2**] = 1.0 × 10⁻⁴ M; [**4**] = 0.50 × 10⁻⁴ M. Kuhn's dissymmetry factors (g_{abs}) at the specified wavelengths are also shown.

region than those of the free ligands, (*R*,*R*)- and (*S*,*S*)-**2**, due to the metal coordination. Hence, the homochiral metallomacrocycles showed mirror image circular dichroism (CD) signals

more intense than those of the free ligands in the longer absorption region with the Kuhn's dissymmetry factor ($|g_{abs}|$) of 2.0×10^{-3} at 332 nm (Fig. 4(iii and iv)) due to the unique chiral metallomacrocyclic structure, which was thermally stable in solution even at 80 °C (Fig. S7, ESI†). (R,R,R,R)-**4** showed a green photoluminescence (PL) band centered at 500 nm in chloroform, which was >100 nm red-shifted from that of the blue emitting (R,R)-**2**, and their fluorescence quantum yields (Φ_F) were determined to be 4 and 13%, respectively (Fig. S8, ESI†). The red-shifted emission band of **4** is most likely attributed to the intramolecular excimer formation between the benzo[f]isoquinoline moieties that is triggered by the close proximity of the two triptycene ligands in the metallomacrocycle (Fig. S9, ESI†). The enantiomeric pairs of **2** and **4** showed weak but mirror-imaged CPL signals with the luminescence dissymmetry factors ($|g_{lum}|$) up to *ca.* 0.4×10^{-3} in the corresponding PL regions (Fig. S8, ESI†).

In summary, we have succeeded in the first synthesis of optically-pure triptycene-based rhombic metallomacrocycles from enantio-pure triptycene-derived ladder-type ligands with a high thermal stability by coordination-driven self-assembly with a *cis*-platinum(II) complex. In addition, we, for the first time, succeeded in the homochiral self-sorting of the racemic triptycene to exclusively produce a pair of enantiomeric homochiral metallomacrocycles. The rigid shape-persistent geometry of the ladder-structured ligand is of key importance for the quantitative and selective metallo-macrocycle formation as well as the homochiral self-sorting. Therefore, the corresponding flexible non-ladder precursor ligands afforded a complicated oligomeric mixture upon mixing with a *cis*-platinum(II) complex. We believe that the present ligand design approach by ladderization of the flexible precursors can be applied to the selective synthesis of a further variety of discrete homochiral metallomacrocycles and cages with different geometry and ring sizes suitable for specific chiral or prochiral guest binding for chiral recognition/separation or asymmetric catalysis in a highly-enantio-selective manner, respectively, based on the rational design of the chiral ladder-structured ligands and proper selection of metal ions.

Conflicts of interest

There are no conflicts to declare.

Notes and references

1 P. D. Bartlett, M. J. Ryan and S. G. Cohen, *J. Am. Chem. Soc.*, 1942, **64**, 2649–2653.
2 A. Sonoda, F. Ogura and M. Nakagawa, *Bull. Chem. Soc. Jpn.*, 1962, **35**, 853–857.
3 G.-W. Zhang, P.-F. Li, Z. Meng, H.-X. Wang, Y. Han and C. F. Chen, *Angew. Chem., Int. Ed.*, 2016, **55**, 5304–5308.
4 F. K.-C. Leung, F. Ishiwari, Y. Shoji, T. Nishikawa, R. Takeda, Y. Nagata, M. Suginome, Y. Uozumi, Y. M. A. Yamada and T. Fukushima, *ACS Omega*, 2017, **2**, 1930–1937.
5 T. Ikai, N. Nagata, S. Awata, Y. Wada, K. Maeda, M. Mizuno and T. M. Swager, *RSC Adv.*, 2018, **8**, 20483–20487.
6 T. Ikai, T. Yoshida, K. Shinohara, T. Taniguchi, Y. Wada and T. M. Swager, *J. Am. Chem. Soc.*, 2019, **141**, 4696–4703.
7 T. Ikai, Y. Wada, S. Awata, C. Yun, K. Maeda, M. Mizuno and T. M. Swager, *Org. Biomol. Chem.*, 2017, **15**, 8440–8447.
8 T. Ikai, T. Yoshida, S. Awata, Y. Wada, K. Maeda, M. Mizuno and T. M. Swager, *ACS Macro Lett.*, 2018, **7**, 364–369.
9 Y. Wada, K. Shinohara and T. Ikai, *Chem. Commun.*, 2019, **55**, 11386–11389.
10 G. Preda, A. Nitti and D. Pasini, *ChemistryOpen*, 2020, **9**, 719–727.
11 M. J. Gu, Y. F. Wang, Y. Han and C. F. Chen, *Org. Biomol. Chem.*, 2021, **19**, 10047–10067.
12 M. N. Khan and T. Wirth, *Chem. – Eur. J.*, 2021, **27**, 7059–7068.
13 C. F. Chen and Y. Han, *Acc. Chem. Res.*, 2018, **51**, 2093–2106.
14 C. Azerraf, S. Cohen and D. Gelman, *Inorg. Chem.*, 2006, **45**, 7010–7017.
15 S. Chakraborty, S. Mondal, Q. J. Li and N. Das, *Tetrahedron Lett.*, 2013, **54**, 1681–1685.
16 A. Dubey, A. Mishra, J. W. Min, M. H. Lee, H. Kim, P. J. Stang and K. W. Chi, *Inorg. Chim. Acta*, 2014, **423**, 326–331.
17 S. Chakraborty, S. Bhowmick, J. Q. Ma, H. W. Tan and N. Das, *Inorg. Chem. Front.*, 2015, **2**, 290–297.
18 A. Vuillamy, S. Zebret, C. Besnard, V. Placide, S. Petoud and J. Hamacek, *Inorg. Chem.*, 2017, **56**, 2742–2749.
19 Y. Sakata, R. Yamamoto, D. Saito, Y. Tamura, K. Maruyama, T. Ogoshi and S. Akine, *Inorg. Chem.*, 2018, **57**, 15500–15506.
20 J. Plutnar, C. Givelet, C. Lemouchi, J. J. Dytrtová, I. Císařová, S. J. Teat and J. Michl, *Organometallics*, 2019, **38**, 4633–4644.
21 S. Hasegawa, S. L. Meichsner, J. J. Holstein, A. Baksi, M. Kasanmascheff and G. H. Clever, *J. Am. Chem. Soc.*, 2021, **143**, 9718–9723.
22 M. M. Safont-Sempere, G. Fernández and F. Würthner, *Chem. Rev.*, 2011, **111**, 5784–5814.
23 H. Jędrzejewska and A. Szumna, *Chem. Rev.*, 2017, **117**, 4863–4899.
24 H. Kar and S. Ghosh, *Isr. J. Chem.*, 2019, **59**, 881–891.
25 S. Hiraoka, *Isr. J. Chem.*, 2019, **59**, 151–165.
26 C. Li, Y. Zuo, Y.-Q. Zhao and S. Zhang, *Chem. Lett.*, 2020, **49**, 1356–1366.
27 Q. Liu, B. Jin, Q. Li, H. Yang, Y. Luo and X. Li, *Soft Matter*, 2022, **18**, 2484–2499.
28 Das and co-workers reported that racemic 2,6-linked triptycene-based organoplatinum complexes self-assembled to form metallo-macrocycles in the presence of disodium terephthalate, but their structures and self-sorting behaviors (homochiral or heterochiral) were not fully elucidated, see: ref 17.
29 P. J. Stang, D. H. Cao, S. Saito and A. M. Arif, *J. Am. Chem. Soc.*, 1995, **117**, 6273–6283.
30 M. B. Goldfinger and T. M. Swager, *J. Am. Chem. Soc.*, 1994, **116**, 7895–7896.
31 M. B. Goldfinger, K. B. Crawford and T. M. Swager, *J. Am. Chem. Soc.*, 1997, **119**, 4578–4593.